

## Accepted version

Int. J. Modelling, Identification and Control, Vol. 33, No. 4, pp.331–343  
Accepted 08/11/2019 DOI:10.1504/IJMIC.2019.107483

# Quasi-Bilinear Modelling and Control of Directional Drilling

Isonguyo J. Inyang

RACE

UK Atomic Energy Authority,

Culham Science Centre,

Abingdon, Oxfordshire, OX14 3ZF, UK

James F Whidborne

School of Aerospace, Transport and Manufacturing,

Cranfield University,

Bedfordshire, MK43 0AL, UK

## Abstract

A Quasi-Bilinear Proportional-plus-Integral (QBPI) controller is proposed for the attitude control of directional drilling tools for the oil and gas industry; and it is designed based on the proposed quasi-bilinear model of the directional drilling tool. The quasi-bilinear model accurately depicts the nonlinear characteristics of the directional drilling tool to a greater extent than the existing linear model, thus extends the scope of appropriate performance. The proposed QBPI control system is an LTI system and it is shown to be exponentially stable. The proposed QBPI controller outstandingly diminishes the deleterious impact of disturbances and measurement delay regarding to performance and stability of the directional drilling tool, and it yields invariant azimuth responses. Drilling cycle scheme which captures the drilling cycle and toolface actuator dynamics of the directional drilling tool, is developed. The servo-velocity and servo-position loops of the toolface servo-control architecture are proven to be robustly stable using Kharitonov's Theorem.

## 1 Introduction

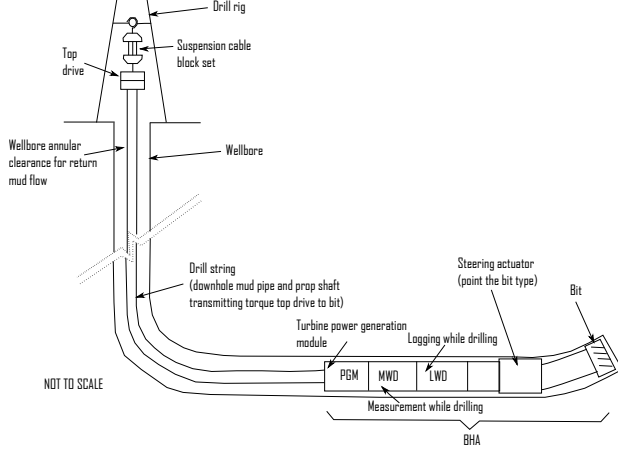
The extension of life of existing oilwells and the exploitation of difficult-to-commercialize and smaller oilwells are currently done by the use of directional drilling tools [Pedersen et al., 2009]. Directional drilling principally requires the control of the inclination and azimuth angles, that is, the attitude control of the directional drilling tool. With the automatic control of the inclination and azimuth angles

of the directional drilling tool, oil and gas production is maximised and the cost per foot of the wellbore is minimised.

The primary elements of a regular directional drilling system are shown in Figure 1. An integral element of the directional drilling system is the Bottom-Hole Assembly (BHA), and it is made up of stabilisers, steering unit (actuator), control unit, Logging While Drilling (LWD) subsystem, Power Generation Module (PGM), Direction and Inclination (D&I) sensor, Measurement While Drilling (MWD) subsystem and other elements. The BHA in combination with the drill pipe is known as drill string. The weight and torque transmission from the top drive (situated at the surface) to the bit (situated underneath the earth's surface) is provided by the drill string. In the course of the propagation of the wellbore, the rocks are crushed by the bit and the lubrication and cooling of the rocks crushing process is done by the drilling mud. Through the drilling string, the drilling mud is transmitted from the surface to the bit and from the bit with the rock-cuttings to the surface through the annulus - the space between the wellbore and the drill string. At the surface, after the rock-cuttings are removed from the drilling mud, the drilling mud is retransmitted. The curvature and direction of the directional drilling tool are changed as required through the steering unit (actuator). The MWD and LWD subsystems handle the assessments, measurements and surveys of physical parameters and formation properties, respectively. More details of the directional drilling system and its functions are provided in Short [1993], Inyang [2017], Devereux [1999] and Baker [1996].

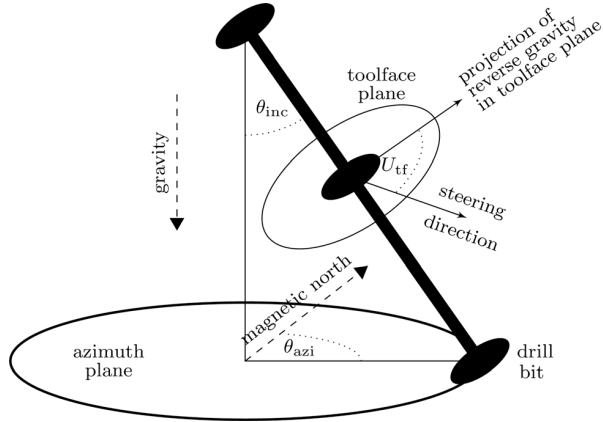
The inclination angle,  $\theta_{inc}$  and azimuth angle,  $\theta_{azi}$

Figure 1: Schematic of a directional drilling system and its primary components



shown in Figure 2 are sensed and measured through the used of D&I sensor. The  $\theta_{inc} \in [0^\circ, 180^\circ]$  denotes the angular deviation from the vertical with  $180^\circ$ ,  $90^\circ$  and  $0^\circ$  corresponding to upward, horizontal and downward, respectively. The  $\theta_{azi} \in [0^\circ, 360^\circ]$  is assessed based on the Earth's magnetic field projection in the horizontal plane, where due West, South, East and North depicts  $270^\circ$ ,  $180^\circ$ ,  $90^\circ$  and  $0^\circ$ , respectively.

Figure 2: Typical steering and attitude parameters of directional drilling tool



During the directional drilling operations, the trajectory and attitude control is done through the implementation of the control algorithms in the control unit. It is noted that communication between the downhole and surface is limited [Inyang and Whidborne, 2019]. Therefore, the implementation of the control algorithms must be done downhole. The well-

bore surrounding is extremely harsh, and could be many kilometres far down from the surface. It is necessitated that the control algorithms have to simple because of the extreme harsh surrounding and restricted power supply.

The design of a general system-independent attitude control algorithm for directional drilling tools is described in this article. In Yonezawa et al. [2002] and Genevois et al. [2003], the need for attitude control of directional drilling tools is elucidated, and control algorithms by holding the toolface angle to control the orientation of the directional drilling tools is proposed. Genevois et al. [2003] elucidated that the azimuth control is the attitude control primary challenge, and that it is necessary for closed-loop “shoot and forget systems”. Several azimuth and inclination control methods highlighted in literature are developed particularly for precise system configurations. For example, Yinghui and Yinao [2000] proposed an Automatic Inclination Controller (AIC) to reduce the number of round trip of the tool orientation and to drill economically; and Kuwana et al. [1994], with the application of double-way telemetry communication connections with the surface, proposed an azimuth and inclination control system. Some recent control algorithms include a Bilinear Proportional plus Integral (BPI) controller [Inyang and Whidborne, 2019], a hybrid method consisting of double automation levels for trajectory control of the tool [Matheus et al., 2014, 2012], a modified Smith predictor-BPI controller [Inyang and Whidborne, 2017], a model-based robust controller [Kremers et al., 2016], a Constant Build Rate (CBR) controller [Panchal et al., 2012], a dynamic state-feedback controller design for 3-D directional drilling systems [van de Wouw et al., 2016], a modified Smith predictor-CBR controller [Inyang et al., 2017], a Discrete Time (DT) controller [Panchal et al., 2012], an optimal  $H_\infty$  controller [Bayliss and Whidborne, 2015], a linear quadratic Gaussian controller [Bayliss et al., 2015] and a robust PI controller [Panchal et al., 2010].

With the application of a first-order Taylor series approximation of nonlinear models at a certain operating point, the dynamics of physical systems are usually modelled as linear models. Clearly, the linear models may be inaccurate when considering a broader operating range as compared to bilinear models which capture the dynamics of the nonlinear systems more accurately (see Inyang and Whidborne [2019], Bruni et al. [1974], Schwarz and Dorissen [1989]). Bilinear models can describe nonlinear characteristics over a broader operating range, therefore, extends the scope of appropriate performance and they are regarded to be outstandingly beneficial in applications to physical

systems [Martineau et al., 2002]. Generally, the state space representation of a Multiple-Input Multiple-Output (MIMO) bilinear system is given as [Kim and Lim, 2003]:

$$\dot{x} = Ax + \left( B + \sum_{i=1}^N x_i M_i \right) u \quad (1)$$

where  $N$  is the number of augmented states and expansion terms,  $u \in \mathbb{R}^{m \times 1}$  is the control vector,  $A, B, C$  and  $M_i$  are constant matrices of appropriate dimensions and  $x \in \mathbb{R}^{n \times 1}$  is the vector of state variables.

In this article, a quasi-bilinear model of the directional drilling tool is developed by applying the polynomialisation technique [Gu, 2011]. Quasi-bilinear system is considered as an approximation of a nonlinear system by a polynomial system and further simplifying it, without loss of generality, by “freezing” a particular term and considering it as a “quasi” bilinearising operating point, thereby resulting to a system which can be expressed in the form of (1). In this case, with the application of the polynomialisation technique, the approximation of the nonlinear system in the polynomial system form is first obtained, and then to further simplify the polynomial system, without loss of generality, a modelling modification is made by considering a particular term as a “quasi” bilinearising operating point to obtain a quasi-bilinear system. For various reasons, various researchers have presented that modelling modification can be done to a system without loss of generality. For example, Tse and Adams [1992] proposed a quasi-linear model of DC-DC converters by considering the perturbation of an approximate large-signal equation around a “varying” operating point in a reduced variable space, White et al. [2007] proposed quasi-LPV model of missile by the inclusion of explicit dependence of the aerodynamic derivatives on the external parameters (roll angle, Mach number) and incidences (state vectors) to the linearised nonlinear model of the missile.

During directional drilling operations, the tool is subjected to time delay on the feedback measurements and disturbances. The lengthy time delay is as a result of the fact that the attitude change of the tool is measured by the D&I sensor and it is, by necessity, situated several distance (usually some tens of feet) behind the bit. The increase of the distance of the bit from the D&I sensor leads to the increase of time delay, and conversely, the increase of the Rate of Penetration (ROP) leads to the decrease of the time delay. While the disturbance arises due to the variation of rock formations, a likelihood for the tool to

drop vertically due to gravity, and to drift towards a horizontal orientation. Though good performance is provided by the PI controller proposed by Panchal et al. [2010] for the attitude control of the directional drilling tool, it is inadequately robust to handle the deleterious impact of the time delay on feedback measurements and disturbances. Also, the PI controller proposed by Panchal et al. [2010] provides inconsistent azimuth responses when it operates beyond its designed operating point.

With the extension of some of the works of Panchal et al. [2010], this article proposes a Quasi-Bilinear Proportional plus Integral (QBPI) controller for the attitude control of the directional drilling tool that is adequately robust to handle the deleterious impact of the time delay on feedback measurements and disturbances. The QBPI controller provides invariant azimuth responses for a broader operating range of the directional drilling tool operations. The simplicity of the QBPI controller makes it easy to implement in directional drilling tools for cost-effective field development, more effective drilling and improved capability of accessing difficult reservoirs.

The remaining part of this article is structured as follows: Section 2 summarises the earlier work; Section 3 presents the development and accuracy of a quasi-bilinear model of the directional drilling tool; Section 4 covers the development of a drilling cycle scheme used for High-Fidelity Model (HFM) simulation analyses, as well as the robust stability analyses of the servo-velocity and servo-position loops of the drilling cycle scheme; Section 5 presents the design of QBPI controller; Section 6 covers the stability analysis of QBPI controller; Section 7 presents the Low-Fidelity Model (LFM) and HFM simulation results; and Conclusions are presented in Section 8.

## 2 Summary of Earlier Work

The model proposed by Panchal et al. [2010] is illustrated in Figure 2 and it is given as:

$$\dot{\theta}_{\text{inc}} = V_{\text{rop}} (U_{\text{dls}} \cos U_{\text{tf}} - V_{\text{dr}}) \quad (2)$$

$$\dot{\theta}_{\text{azi}} = \frac{V_{\text{rop}}}{\sin \theta_{\text{inc}}} (U_{\text{dls}} \sin U_{\text{tf}} - V_{\text{tr}}) \quad (3)$$

and with the application of control transformation given as:  $U_{\text{dls}} = K_{\text{dls}} \sqrt{(U_{\text{azi}})^2 + (U_{\text{inc}})^2}$  and  $U_{\text{tf}} = \text{ATAN2}(U_{\text{azi}}, U_{\text{inc}})$ , the model, (2) and (3) is partially linearised and decoupled as follows [Panchal et al.,

2010]:

$$\dot{\theta}_{\text{inc}} = V_{\text{rop}} K_{\text{dls}} U_{\text{inc}} \quad (4)$$

$$\dot{\theta}_{\text{azi}} = \frac{V_{\text{rop}}}{\sin \theta_{\text{inc}}} K_{\text{dls}} U_{\text{azi}} \quad (5)$$

where  $\theta_{\text{azi}}$  is the azimuth angle,  $U_{\text{tf}}$  is the toolface angle control input,  $K_{\text{dls}}$  is the open-loop curvature capability of the tool,  $U_{\text{inc}}$  is the virtual control inclination,  $V_{\text{dr}} = \alpha \sin \theta_{\text{inc}}$ ,  $U_{\text{dls}}$  is the curvature, also known as “dogleg severity” which is the product of duty cycle and  $K_{\text{dls}}$ ,  $\alpha$  is a constant,  $U_{\text{azi}}$  is the virtual control for the azimuth,  $V_{\text{tr}}$  is the turn rate bias disturbance,  $V_{\text{rop}}$  is the rate of penetration, a time-varying parameter, and  $\theta_{\text{inc}}$  is the inclination angle. Matheus et al. [2014, 2012] (see also Cockburn et al. [2011], Matheus and Naganathan [2010]) have also used the model, (2) and (3) in their work with the presentation of field tested results to show the fidelity of the model.

Based on kinematic considerations of directional drilling tool, the model, (2) and (3) is derived. It does not take into consideration the lateral and torsional dynamics of the BHA and drillstem. Also, it does not take into consideration the drilling cycle and toolface actuator dynamics, hence, in Section 4, a drilling cycle scheme which captures the drilling cycle and toolface actuator dynamics is developed and is used for HFM simulation analyses in Section 7. Note that in (3) there is a singularity when  $\theta_{\text{inc}} = 0^\circ$ , hence, the model, (2) and (3) is limited to attitudes such that  $\theta_{\text{inc}}$  is not close to  $0^\circ$ .

### 3 Quasi-Bilinear Model of Directional Drilling Tool

In this section, the polynomialisation technique [Gu, 2011] is applied to the partially linearised and decoupled system, (4) and (5), to obtain a quasi-bilinear model of the directional drilling tool. As presented in the remainder of this section, with the application of the polynomialisation technique, the approximation of (4) and (5) in the polynomial system form is first obtained, and then to further simplify the polynomial system, without loss of generality, a modelling modification is made by considering a particular term as a “quasi” bilinearising operating point to obtain a quasi-bilinear system.

Polynomialisation technique is applied to (4) and

(5) by introducing the following state variables:

$$\begin{aligned} x_1 &= \theta_{\text{inc}} \\ x_2 &= \theta_{\text{azi}} \\ x_3 &= \frac{1}{\sin(\theta_{\text{inc}})} \\ x_4 &= \sin(\theta_{\text{inc}}) \\ x_5 &= \cos(\theta_{\text{inc}}) \end{aligned} \quad (6)$$

Differentiating (6) with respect to time and substituting (4), (5) and (6), the following is obtained:

$$\begin{aligned} \dot{x}_1 &= \dot{\theta}_{\text{inc}} = a U_{\text{inc}} \\ \dot{x}_2 &= \dot{\theta}_{\text{azi}} = a x_3 U_{\text{azi}} \\ \dot{x}_3 &= -\frac{1}{[\sin(\theta_{\text{inc}})]^2} \dot{\theta}_{\text{inc}} \cos(\theta_{\text{inc}}) = -a \hat{x}_3^2 x_5 U_{\text{inc}} \\ \dot{x}_4 &= \dot{\theta}_{\text{inc}} \cos(\theta_{\text{inc}}) = a x_5 U_{\text{inc}} \\ \dot{x}_5 &= -\dot{\theta}_{\text{inc}} \sin(\theta_{\text{inc}}) = -a x_4 U_{\text{inc}} \end{aligned} \quad (7)$$

where  $a = V_{\text{rop}} K_{\text{dls}}$ ,  $\hat{x}_3^2$  is considered as a “quasi” bilinearising operating point for  $x_3$ , that is,  $\hat{x}_3^2 = \pi/2$ . Therefore, the following quasi-bilinear system is obtained:

$$\begin{aligned} \dot{x}_1 &= a U_{\text{inc}} \\ \dot{x}_2 &= a x_3 U_{\text{azi}} \\ \dot{x}_3 &= -(\pi/2) a x_5 U_{\text{inc}} \\ \dot{x}_4 &= a x_5 U_{\text{inc}} \\ \dot{x}_5 &= -a x_4 U_{\text{inc}} \end{aligned} \quad (8)$$

and (8) is expressed in the form of (1) as:

$$\dot{x} = Ax + (B + x_3 M_3 + x_5 (M_A + M_B) + x_4 M_4) u$$

where  $A = [ ]$ ,  $M_1 = [ ]$ ,  $M_2 = [ ]$ ,  $M_5 = M_A + M_B$ ,  $u = [U_{\text{inc}}, U_{\text{azi}}]^T$  and:

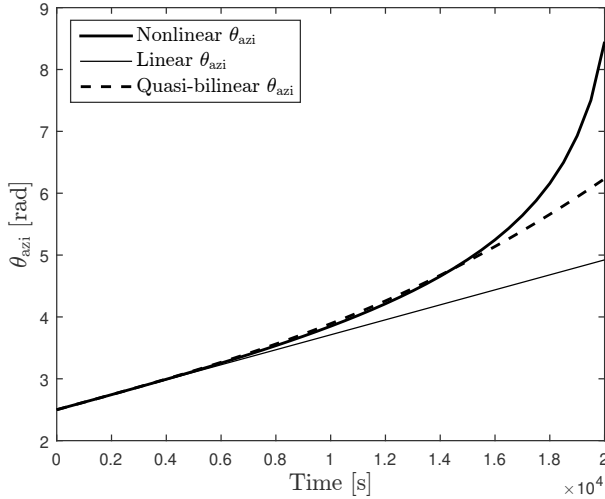
$$\begin{aligned} B &= \begin{bmatrix} a & 0 \\ 0 & 0 \\ 0 & 0 \\ 0 & 0 \\ 0 & 0 \end{bmatrix}, \quad M_3 = \begin{bmatrix} 0 & 0 \\ a & 0 \\ 0 & 0 \\ 0 & 0 \\ 0 & 0 \end{bmatrix}, \quad M_A = \begin{bmatrix} 0 & 0 \\ 0 & 0 \\ -(\pi/2)a & 0 \\ 0 & 0 \\ 0 & 0 \end{bmatrix} \\ M_B &= \begin{bmatrix} 0 & 0 \\ 0 & 0 \\ 0 & 0 \\ a & 0 \\ 0 & 0 \end{bmatrix}, \quad M_4 = \begin{bmatrix} 0 & 0 \\ 0 & 0 \\ 0 & 0 \\ 0 & 0 \\ -a & 0 \end{bmatrix} \end{aligned} \quad (9)$$

The proposed quasi-bilinear model is used as the basis for the QBPI controller design as analysed in Section 5. In the remaining part of this section, the accuracy of the proposed quasi-bilinear model of the directional drilling tool is analysed.

### 3.1 Quasi-Bilinear Model Accuracy

The accuracy of the proposed quasi-bilinear model of the directional drilling tool is demonstrated through the analysis of the transient azimuth responses for the open-loop systems using the proposed quasi-bilinear model and comparing with those from the linear model and nonlinear model, (2) and (3) (with  $V_{dr}$  and  $V_{tr}$  ignored) proposed by Panchal et al. [2010]. Given that there is no nonlinearity in the inclination open-loops of the models, the inclination responses of the models are expected to be identical. The models comparison simulation parameters are as follows:  $K_{dls} = 10^\circ/100$  ft,  $V_{rop} = 100$  ft/hr and  $\theta_{azi} = 2.5$  rad.

Figure 3: Comparison of azimuth responses of quasi-bilinear, linear and nonlinear models



The comparison of the azimuth responses of the proposed quasi-bilinear, linear (proposed by Panchal et al. [2010]) and nonlinear ((2) and (3) with  $V_{dr}$  and  $V_{tr}$  ignored) models of the directional drilling tool are shown in Figure 3. Based on Figure 3, the azimuth responses of the proposed quasi-bilinear model converges more closely to the azimuth response of the nonlinear model than that of the linear model. Therefore, the proposed quasi-bilinear model depicts the nonlinear model more correctly than the linear model proposed by Panchal et al. [2010], hence widening the degree of appropriate performances, and it is considered to be outstandingly beneficial in applications to directional drilling operations.

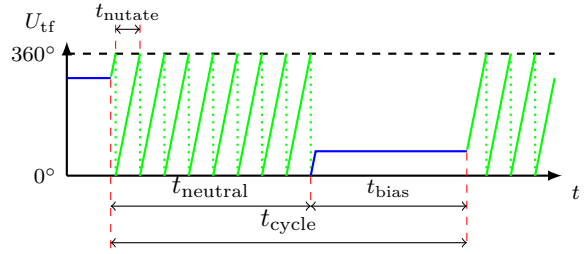
## 4 Drilling Cycle Scheme

This section presents the development of a drilling cycle scheme for the directional drilling tool model, (2) and (3). The developed drilling cycle scheme captures the drilling cycle and toolface actuator dynamics, and it is used in Section 7 for the HFM simulation analyses. Here, the developed drilling cycle scheme has a toolface servo-control architecture which is a combination of servo-position and servo-velocity loops.

During directional drilling operations, directional drilling tools in point-the-bit and push-the-bit steering assembly varieties steer by the application of a constant force against the formation or by having a fixed bend. With the continuous rotation of the steering assembly of the directional drilling tool, straight-hole sections are formed. Sections of wellbores with variable curvature,  $U_{dls}$  less than the maximum curvature,  $K_{dls}$ , that is,  $U_{dls} \leq K_{dls}$  can be achieved [Panchal et al., 2011]. To engineer the  $U_{dls}$  of the system given by (2) and (3), the toolface actuation,  $U_{tf}$  (control input) is discretised into duty cycles known as “drilling cycles” of period,  $t_{cycle}$ . To approximate the  $U_{dls}$  control input,  $t_{cycle}$  is proportioned into the bias,  $t_{bias}$  and neutral,  $t_{neutral}$  phases as shown in Figure 4. In the  $t_{neutral}$  phase, the  $U_{tf}$  is cycled at a constant rate of period,  $t_{nutate}$ ; while in the  $t_{bias}$  phase, the  $U_{tf}$  is a servo-controlled constant which approximates the  $U_{dls}$  control input as:

$$U_{dls} = \frac{t_{bias}}{t_{cycle}} K_{dls} \quad (10)$$

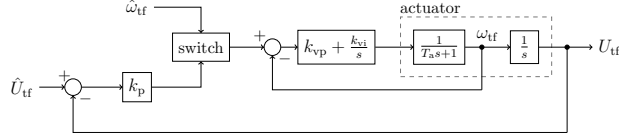
Figure 4: Drilling cycle definition



The toolface is driven by a servo mechanism; hence, the toolface response to demands in the tool is subject to lag dynamics. The servo-control architecture is shown in Figure 5, where  $\hat{\omega}_{tf}$  is the constant nutate rate demand,  $\hat{U}_{tf}$  is the required toolface angle,  $T_a$  is the time constant of the servo loop,  $k_p$  is the proportional term in servo-position loop, and the proportional and integral term in the servo-velocity loop are  $k_{vp}$  and  $k_{vi}$ , respectively.

The servo operates as a position control in the bias phase and as a speed control in the neutral phase. Integral action is placed in the velocity loop to ensure accurate rotation speed of the toolface in the neutral phase, which means that integral action is not required in the outer loop position-control loop; therefore, a proportional controller is used. This method has an added advantage of removing the need for antiwindup and bump-free transfer for the switching between position and velocity tracking.

Figure 5: Toolface servo-control architecture for drilling cycle scheme



The toolface controller switch operates such that during the neutral phase,  $\hat{\omega}_{tf}$  is applied to the servo-control system velocity demand. During the bias phase,  $\hat{U}_{tf}$  is applied to the servo-control system angle position demand.

As shown in Figure 6, at the conclusion of the neutral phase, there is a difference between the required toolface angle and the actual toolface angle. Hence, at the beginning of the drilling cycle, there is a change to time,  $\Delta t_{neutral}$  when the switch from  $t_{neutral}$  to  $t_{bias}$  is calculated. From Figure 6, the calculation is straightforward and given by:

$$\Delta t_{neutral} = \frac{\Delta \hat{U}_{tf}}{\hat{\omega}_{tf}} \quad (11)$$

where  $\Delta \hat{U}_{tf} \in [-\pi, \pi)$  is the toolface correction angle given by:

$$\Delta \hat{U}_{tf} = \alpha_{tf} - 2\pi(\text{round}(\alpha_{tf}/(2\pi))) \quad (12)$$

where

$$\alpha_{tf} = \hat{\omega}_{tf} t_{neutral} - \hat{U}_{tf}(k) + \hat{U}_{tf}(k-1) \quad (13)$$

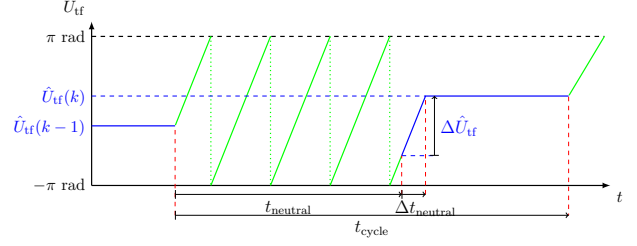
$\hat{U}_{tf}(k)$  represents the toolface demand for the current ( $k$ th) drilling cycle, and  $\hat{U}_{tf}(k-1)$  represents the toolface demand for the previous ( $(k-1)$ th) drilling cycle.

The developed drilling cycle scheme is implemented with the system given by (2) and (3) for the HFM simulations analyses with respect to the attitude control of the directional drilling tool in Subsection 7.2.

#### 4.1 Robust Stability Analysis of Servo-Velocity Loop

To analyse the stability of the servo-velocity loop of the toolface servo-control architecture, Kharitonov's

Figure 6: Calculation of  $\Delta t_{neutral}$  for  $k$ th drilling cycle



Theorem [Kharitonov, 1978] (see Theorem 4.1) is applied. Kharitonov's Theorem is used for the robust stability analysis of an uncertain controlled system through the definition of four bounding polynomials and testing each of them with Routh-Hurwitz criterion [Routh, 1905]. It provides a required and adequate form for all polynomials in a particular group to be Hurwitz stable [Callier and Desoer, 1991].

Considering an interval polynomial given as:

$$P(s) = a_0 s^0 + a_1 s^1 + a_2 s^2 + a_3 s^3 + \dots + a_n s^n \quad (14)$$

where  $a_i \in \mathbb{R}$ ,  $a_i \in [\underline{a}_i, \bar{a}_i]$  for all  $i = 0, 1, \dots, n$ ;  $a_i$  are the coefficients of the interval polynomial;  $\underline{a}_i$  and  $\bar{a}_i$  are the minimum and maximum values of  $a_i$ , respectively. It is assumed that the minimum and maximum values of the coefficient of the highest order of the polynomial,  $\underline{a}_n$  and  $\bar{a}_n$  cannot be zero. Kharitonov's Theorem is stated as follows:

**Theorem 4.1** [Kharitonov, 1978]. *The interval polynomial, (14) is robustly stable if and only if the four Kharitonov polynomials*

$$P_1(s) = \underline{a}_0 s^0 + \underline{a}_1 s^1 + \bar{a}_2 s^2 + \bar{a}_3 s^3 + \underline{a}_4 s^4 + \underline{a}_5 s^5 + \dots \quad (15)$$

$$P_2(s) = \bar{a}_0 s^0 + \bar{a}_1 s^1 + \underline{a}_2 s^2 + \underline{a}_3 s^3 + \bar{a}_4 s^4 + \bar{a}_5 s^5 + \dots \quad (16)$$

$$P_3(s) = \underline{a}_0 s^0 + \bar{a}_1 s^1 + \bar{a}_2 s^2 + \underline{a}_3 s^3 + \underline{a}_4 s^4 + \bar{a}_5 s^5 + \dots \quad (17)$$

$$P_4(s) = \bar{a}_0 s^0 + \underline{a}_1 s^1 + \underline{a}_2 s^2 + \bar{a}_3 s^3 + \bar{a}_4 s^4 + \underline{a}_5 s^5 + \dots \quad (18)$$

are stable.

With the application of Routh-Hurwitz criterion [Routh, 1905] or any other technique, the stability of the four Kharitonov polynomials can be analysed.

The servo-velocity loop of the toolface servo-control architecture is shown in Figure 7. Based on Figure 7,

the closed-loop output response is given as:

$$\omega_{\text{tf}} = \frac{k_{\text{vp}}s + k_{\text{vi}}}{T_a s^2 + (1 + k_{\text{vp}})s + k_{\text{vi}}} \hat{\omega}_{\text{tf}} \quad (19)$$

From (19), the closed-loop characteristic equation is given as:

$$T_a s^2 + (1 + k_{\text{vp}})s + k_{\text{vi}} = 0 \quad (20)$$

With reference to Theorem 4.1, (20) is in the form of

$$P(s) = a_2 s^2 + a_1 s + a_0 \quad (21)$$

with

$$a_2 = T_a \quad (22)$$

$$a_1 = 1 + k_{\text{vp}} \quad (23)$$

$$a_0 = k_{\text{vi}} \quad (24)$$

If the parameters of (20) are bounded as  $T_a \in [\underline{T}_a, \bar{T}_a]$ ,  $k_{\text{vp}} \in [\underline{k}_{\text{vp}}, \bar{k}_{\text{vp}}]$  and  $k_{\text{vi}} \in [\underline{k}_{\text{vi}}, \bar{k}_{\text{vi}}]$  with

$$T_a, k_{\text{vp}}, k_{\text{vi}} > 0 \quad (25)$$

then the bounded coefficients, (22)-(24) are obtained as  $a_2 \in [\underline{a}_2, \bar{a}_2]$ ,  $a_1 \in [\underline{a}_1, \bar{a}_1]$  and  $a_0 \in [\underline{a}_0, \bar{a}_0]$  where

$$\underline{a}_2 = \underline{T}_a \quad (26)$$

$$\bar{a}_2 = \bar{T}_a \quad (27)$$

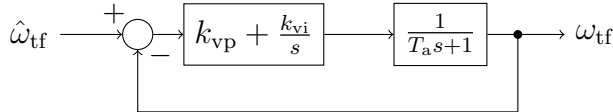
$$\underline{a}_1 = 1 + \underline{k}_{\text{vp}} \quad (28)$$

$$\bar{a}_1 = 1 + \bar{k}_{\text{vp}} \quad (29)$$

$$\underline{a}_0 = \underline{k}_{\text{vi}} \quad (30)$$

$$\bar{a}_0 = \bar{k}_{\text{vi}} \quad (31)$$

Figure 7: Servo-velocity loop of toolface servo-control architecture



With practical engineering considerations of the servo-velocity loop, and to analyse the robust stability of the servo-velocity loop, the parameters of (20) are considered to be bounded and also satisfy the conditions of (25) as  $T_a \in [0.5, 3]$  s,  $k_{\text{vp}} \in [0.25, 0.7]$  and  $k_{\text{vi}} \in [3, 6]$  s<sup>-1</sup>, and based on (26)-(31), the bounded coefficients, (22)-(24) are obtained as  $a_2 \in [0.5, 3]$  s,  $a_1 \in [1.25, 1.7]$  and  $a_0 \in [3, 6]$  s<sup>-1</sup>. Therefore, the four Kharitonov polynomials are given

as:

$$P_1(s) = 3s^2 + 1.25s + 3 \quad (32)$$

$$P_2(s) = 0.5s^2 + 1.7s + 6 \quad (33)$$

$$P_3(s) = 3s^2 + 1.7s + 3 \quad (34)$$

$$P_4(s) = 0.5s^2 + 1.25s + 6 \quad (35)$$

The Routh-Hurwitz criterion [Routh, 1905] is used to test the stability of the Kharitonov polynomials, (32) - (35). Thus, Routh tables for the Kharitonov polynomials, (32) - (35) are created as shown in Table 1. Based on the analyses of Table 1, the Kharitonov polynomials  $P_1(s)$ ,  $P_2(s)$ ,  $P_3(s)$  and  $P_4(s)$  of (32) - (35), respectively, are stable. Therefore, the servo-velocity loop of the toolface servo-control architecture is robustly stable.

Table 1: Routh Tables for Kharitonov Polynomials (32)-(35)

$P_1(s)$			$P_2(s)$		
$s^2$	3	3	$s^2$	0.5	6
$s^1$	1.25	0	$s^1$	1.7	0
$s^0$	3	0	$s^0$	6	0

$P_3(s)$			$P_4(s)$		
$s^2$	3	3	$s^2$	0.5	6
$s^1$	1.7	0	$s^1$	1.25	0
$s^0$	3	0	$s^0$	6	0

## 4.2 Robust Stability Analysis of Servo-Position Loop

Similar to Subsection 4.1, the stability of the servo-position loop of the toolface servo-control architecture is analysed by applying Theorem 4.1. The servo-position loop of the toolface servo-control architecture is shown in Figure 8.

Based on Figure 8, the closed-loop output response is given as:

$$U_{\text{tf}} = \frac{(k_{\text{vp}}s + k_{\text{vi}})k_{\text{p}}}{T_a s^3 + (1 + k_{\text{vp}})s^2 + (k_{\text{vi}} + k_{\text{vp}}k_{\text{p}})s + k_{\text{vi}}k_{\text{p}}} \hat{U}_{\text{tf}} \quad (36)$$

From (36), the closed-loop characteristic equation is given as:

$$T_a s^3 + (1 + k_{\text{vp}})s^2 + (k_{\text{vi}} + k_{\text{vp}}k_{\text{p}})s + k_{\text{vi}}k_{\text{p}} = 0 \quad (37)$$

With reference to Theorem 4.1, (37) is in the form of

$$P(s) = a_3 s^3 + a_2 s^2 + a_1 s + a_0 \quad (38)$$

with

$$a_3 = T_a \quad (39)$$

$$a_2 = 1 + k_{vp} \quad (40)$$

$$a_1 = k_{vi} + k_{vp}k_p \quad (41)$$

$$a_0 = k_{vi}k_p \quad (42)$$

If the parameters of (37) are bounded as  $T_a \in [\underline{T}_a, \bar{T}_a]$ ,  $k_{vp} \in [\underline{k}_{vp}, \bar{k}_{vp}]$ ,  $k_{vi} \in [\underline{k}_{vi}, \bar{k}_{vi}]$  and  $k_p \in [\underline{k}_p, \bar{k}_p]$  with

$$T_a, k_{vp}, k_{vi}, k_p > 0 \quad (43)$$

then the bounded coefficients, (39)-(42) are obtained as  $a_3 \in [\underline{a}_3, \bar{a}_3]$ ,  $a_2 \in [\underline{a}_2, \bar{a}_2]$ ,  $a_1 \in [\underline{a}_1, \bar{a}_1]$  and  $a_0 \in [\underline{a}_0, \bar{a}_0]$  where

$$\underline{a}_3 = \underline{T}_a \quad (44)$$

$$\bar{a}_3 = \bar{T}_a \quad (45)$$

$$\underline{a}_2 = 1 + \underline{k}_{vp} \quad (46)$$

$$\bar{a}_2 = 1 + \bar{k}_{vp} \quad (47)$$

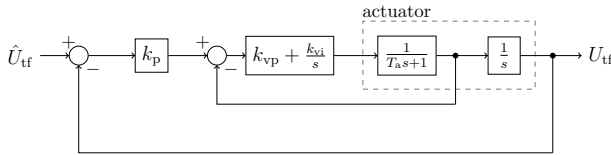
$$\underline{a}_1 = \underline{k}_{vi} + \underline{k}_{vp}\underline{k}_p \quad (48)$$

$$\bar{a}_1 = \bar{k}_{vi} + \bar{k}_{vp}\bar{k}_p \quad (49)$$

$$\underline{a}_0 = \underline{k}_{vi}\underline{k}_p \quad (50)$$

$$\bar{a}_0 = \bar{k}_{vi}\bar{k}_p \quad (51)$$

Figure 8: Servo-position loop of toolface servo-control architecture



With practical engineering considerations of the servo-position loop, and to analyse the robust stability of the servo-position loop, the parameters of (37) are considered to be bounded and also satisfy the conditions of (43) as  $T_a \in [0.5, 3]$  s,  $k_{vp} \in [0.25, 0.7]$ ,  $k_p \in [0.2, 0.42]$  s<sup>-1</sup> and  $k_{vi} \in [3, 6]$  s<sup>-1</sup>, and based on (44) - (51), the bounded coefficients, (39)-(42) are obtained as  $a_3 \in [0.5, 3]$  s,  $a_2 \in [1.25, 1.7]$ ,  $a_1 \in [3.05, 6.294]$  s<sup>-1</sup> and  $a_0 \in [0.6, 1.26]$  s<sup>-1</sup>. Therefore, the four Kharitonov polynomials are given as:

$$P_1(s) = 3s^3 + 1.7s^2 + 3.05s + 0.6 \quad (52)$$

$$P_2(s) = 0.5s^3 + 1.25s^2 + 6.294s + 1.26 \quad (53)$$

$$P_3(s) = 0.5s^3 + 1.7s^2 + 6.294s + 0.6 \quad (54)$$

$$P_4(s) = 3s^3 + 1.25s^2 + 3.05s + 1.26 \quad (55)$$

The Routh-Hurwitz criterion [Routh, 1905] is used to test the stability of the Kharitonov polynomials, (52) - (55). Thus, Routh tables for the Kharitonov polynomials, (52) - (55) are created as shown in Table 2. Based on the analyses of Table 2, the Kharitonov polynomials  $P_1(s)$ ,  $P_2(s)$ ,  $P_3(s)$  and  $P_4(s)$  of (52) - (55), respectively, are stable. Therefore, the servo-position loop of the toolface servo-control architecture is robustly stable.

Table 2: Routh Tables for Kharitonov Polynomials, (52) - (55)

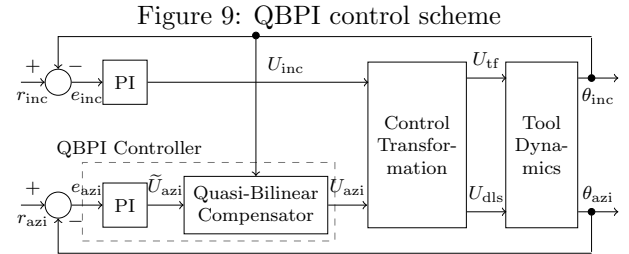
$P_1(s)$			$P_2(s)$		
$s^3$	3	3.05	$s^3$	0.5	6.294
$s^2$	1.7	0.6	$s^2$	1.25	1.26
$s^1$	1.991	0	$s^1$	5.79	0
$s^0$	0.6	0	$s^0$	1.26	0

$P_3(s)$			$P_4(s)$		
$s^3$	0.5	6.294	$s^3$	3	3.05
$s^2$	1.7	0.6	$s^2$	1.25	1.26
$s^1$	6.118	0	$s^1$	0.026	0
$s^0$	0.6	0	$s^0$	1.26	0

## 5 QBPI Controller Design

The proposed QBPI controller design scheme is based on the works of Inyang and Whidborne [2019], and it is a combination of a standard linear PI controller and a quasi-bilinear compensator, as shown in Figure 9. To deal with the nonlinear  $1/\sin \theta_{inc}$  term in (3), the quasi-bilinear compensator is only incorporated in the azimuth feedback loop.



### 5.1 PI Controller

Similar to the works of Inyang and Whidborne [2019], the PI control for the inclination and azimuth control



channels are as follows, respectively:

$$U_{\text{inc}} = k_{\text{pi}}e_{\text{inc}} + k_{\text{ii}} \int_0^t e_{\text{inc}} dt \quad (56)$$

$$\tilde{U}_{\text{azi}} = k_{\text{pa}}e_{\text{azi}} + k_{\text{ia}} \int_0^t e_{\text{azi}} dt \quad (57)$$

where  $k_{\text{pi}}$  and  $k_{\text{pa}}$  are the proportional gains in the inclination and azimuth feedback loops, respectively;  $k_{\text{ii}}$  and  $k_{\text{ia}}$  are the integral gains for the inclination and azimuth feedback loops, respectively;  $e_{\text{azi}} = r_{\text{azi}} - \theta_{\text{azi}}$  and  $e_{\text{inc}} = r_{\text{inc}} - \theta_{\text{inc}}$ ;  $r_{\text{azi}}$  and  $r_{\text{inc}}$  are the nominal operating points for azimuth and inclination, respectively;  $\tilde{U}_{\text{azi}}$  is the control input to the quasi-bilinear compensator. With practical engineering considerations, the PI controllers gains in the azimuth and inclination feedback loops are tuned manually to attain required performance with reference to minimal overshoot, fast settling time and zero steady state error.

## 5.2 Quasi-Bilinear Compensator

With the assumption that in Figure 9,  $U_{\text{azi}} = \tilde{U}_{\text{azi}}$ , then only the PI controller is incorporated (see (57)), and the azimuth feedback loop is expressed as follows:

$$\dot{\theta}_{\text{azi}} = a \frac{1}{\sin \theta_{\text{inc}}} (k_{\text{pa}}e_{\text{azi}} + k_{\text{ia}} \int_0^t e_{\text{azi}} dt) \quad (58)$$

Based on (6) and (8), (58) can further be expressed as:

$$\dot{\theta}_{\text{azi}} = ax_3(k_{\text{pa}}e_{\text{azi}} + k_{\text{ia}} \int_0^t e_{\text{azi}} dt) \quad (59)$$

To deal with the nonlinearity in (59), a quasi-bilinear compensator is proposed for the azimuth feedback loop which is given by:

$$\frac{U_{\text{azi}}}{\tilde{U}_{\text{azi}}} = \frac{1}{x_3} \quad (60)$$

where  $x_3$  is defined based on (8) as follows:

$$x_3 = -(\pi/2)\theta_{\text{inc}} \int_0^t x_5 dt \quad (61)$$

Note that the nonlinearity of  $1/\sin \theta_{\text{inc}}$  in (58) can be accounted for by introducing  $\sin \theta_{\text{inc}}$  as the compensator. However, (60), defined based on states (variables), is applied, which acts as the  $\sin \theta_{\text{inc}}$ ; thereby, simplifying and replacing the trigonometry function.

Furthermore, note that when  $\theta_{\text{inc}} = 0^\circ$ , then  $x_3 = 0$  and there is a singularity in (60). Nonetheless, as previously highlighted in Section 2, there is also a singularity in (3) when  $\theta_{\text{inc}} = 0^\circ$ . Therefore, the proposed QBPI controller is limited to attitudes such that  $\theta_{\text{inc}}$  is not close to  $0^\circ$ .

The quasi-bilinear compensator increases the performance of the PI controller. The quasi-bilinear compensator, in combination with PI controller, enables the ensuing QBPI controller to sustain a desired level of control throughout a wider range of operation.

The proposed QBPI controller is reasonably simple and it can with ease be applied in the directional drilling tools for more effective drilling, field development and the improvement of the potential of accessing difficult reservoirs.

## 6 Stability Analysis of QBPI Controller

With the introduction of augmented states,  $e_{ai}$  and  $e_{aa}$ , representing the accumulated inclination and azimuth errors, respectively, and based on Figure 10, the proposed QBPI control system is written as:

$$\dot{e}_{ai}(t) = -\theta_{\text{inc}}(t) \quad (62)$$

$$\dot{\theta}_{\text{inc}}(t) = (k_{\text{ii}}e_{ai}(t) - k_{\text{pi}}\theta_{\text{inc}}(t))a \quad (63)$$

$$\dot{e}_{aa}(t) = -\theta_{\text{azi}}(t) \quad (64)$$

$$\dot{\theta}_{\text{azi}}(t) = \frac{(k_{\text{ia}}e_{aa}(t) - k_{\text{pa}}\theta_{\text{azi}}(t))a}{x_3(t) \cos \beta(t)} \quad (65)$$

where  $e_{ai}(t)$ ,  $\theta_{\text{inc}}(t)$ ,  $e_{aa}(t)$ ,  $\theta_{\text{azi}}(t) \in \mathbb{R}^n$  and  $t \in \mathbb{R}^+$ . With reference to Figure 10, and based on (4) and (5),  $f_{\text{azi}}(U_{\text{inc}}) = aU_{\text{inc}} = V_{\text{top}}K_{\text{dls}}U_{\text{inc}}$  and  $f_{\text{azi}}(U_{\text{azi}}, \beta) = aU_{\text{azi}}/\cos \beta(t)$  (recall,  $\beta(t) = \pi/2 - \theta_{\text{inc}}(t)$ ), and  $K_q(\tilde{U}_{\text{azi}}, \beta)$  is given in (60).

Recall, from (6),  $x_3(t) = 1/\sin \theta_{\text{inc}}(t) = 1/\cos \beta(t)$ , and with its substitution in (65) for  $\beta(t) \in (-\pi/2, \pi/2)$ , (62)-(65) become:

$$\dot{e}_{ai}(t) = -\theta_{\text{inc}}(t) \quad (66)$$

$$\dot{\theta}_{\text{inc}}(t) = k_{\text{ii}}ae_{ai}(t) - k_{\text{pi}}a\theta_{\text{inc}}(t) \quad (67)$$

$$\dot{e}_{aa}(t) = -\theta_{\text{azi}}(t) \quad (68)$$

$$\dot{\theta}_{\text{azi}}(t) = k_{\text{ia}}ae_{aa}(t) - k_{\text{pa}}a\theta_{\text{azi}}(t) \quad (69)$$

Note that (66)-(69) is a Linear Time Invariant (LTI) system and it can be put in the form of:

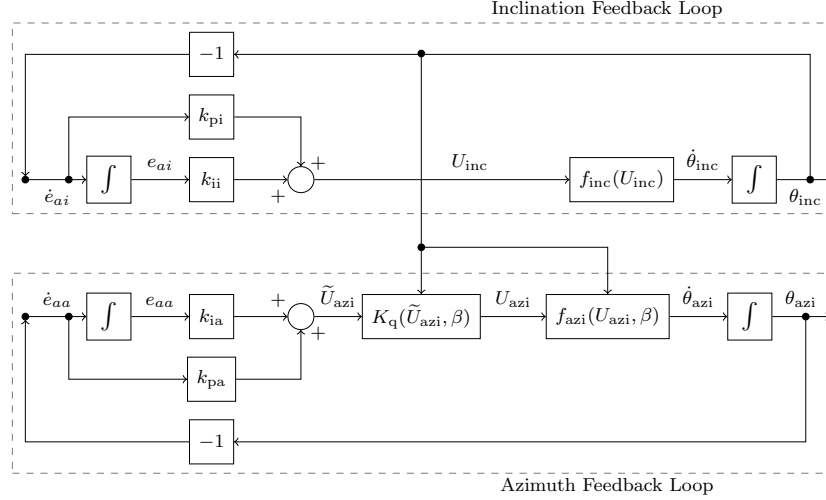
$$\dot{x}(t) = Ax(t), \quad t \geq 0 \quad (70)$$

$$x(0) = x_0$$

where  $x \in \mathbb{R}^n$  denotes the system state,  $A \in \mathbb{R}^{n \times n}$  denotes system matrix, with  $x(t) = [e_{ai}(t), \theta_{\text{inc}}(t), e_{aa}(t), \theta_{\text{azi}}(t)]^T$  and

$$A = \begin{bmatrix} 0 & -1 & 0 & 0 \\ k_{\text{ii}}a & -k_{\text{pi}}a & 0 & 0 \\ 0 & 0 & 0 & -1 \\ 0 & 0 & k_{\text{ia}}a & -k_{\text{pa}}a \end{bmatrix} \quad (71)$$

Figure 10: QBPI control system with augmented states



The eigenvalues of  $A$  are left-half-plane for all positive  $a$ ,  $k_{ia}$ ,  $k_{pa}$ ,  $k_{ii}$  and  $k_{pi}$ ; hence the proposed QBPI control system given in (71) is exponentially stable.

which is given by

$$\tau_d = \frac{d_t}{V_{rop}} \quad (72)$$

where  $d_t$  is the distance of the bit from the D&I sensor.

## 7 Simulation Results

In this section, the transient simulations are carried out using MATLAB/Simulink. The stability, robustness and effectiveness of the proposed QBPI controller are analysed through the transient responses for the closed-loop controlled system using two models, Low-Fidelity Model (LFM) and HFM. The LFM and HFM schemes for the proposed QBPI controller are shown in Figures 11 and 17, respectively. For the LFM simulation scheme, the nonlinear system given by (2) and (3), the proposed QBPI controller and the systems delays are implemented. While the HFM simulation scheme is similar to the LFM simulation scheme but with the implementation of the drilling cycle scheme developed in Section 4. Based on the LFM, simulation results for a variety of responses under different operating conditions are analysed and compared with those from the PI controller of Panchal et al. [2010]. With the implementation of the drilling cycle scheme, the HFM simulation results are analysed to further show that the proposed QBPI controller still holds the inclination and azimuth at the desired angles.

To analyse the adverse effects of disturbances and time delay on the feedback measurements with respect to the stability and performance of the directional drilling tool, the disturbances are implemented as  $V_{dr}$  and  $V_{tr}$  (see (2) and (3)), and the system delays are implemented as  $e^{-\tau_d s}$ , where  $\tau_d$  is time delay

### 7.1 Low-Fidelity Model Simulation

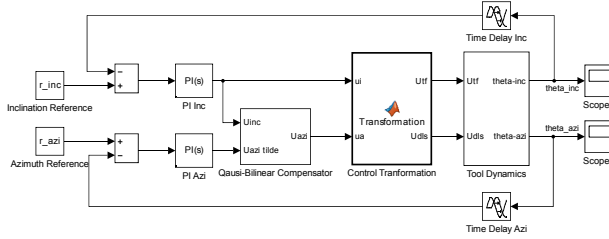
Applying the systems delays, the proposed QBPI controller and the nonlinear system, (2) and (3), MATLAB/Simulink transient simulations are developed with reference to the LFM scheme (see Figure 11), to investigate the stability, robustness and effectiveness of the proposed QBPI controller over the PI controller proposed by Panchal et al. [2010]. The LFM simulations parameters are presented in Table 3 and they are dependent on practical engineering considerations. The saturation effect is removed for the reason of viewing the dynamic responses. To analyse the invariance of the azimuth responses of the proposed QBPI controller compared to those of the PI controller proposed by Panchal et al. [2010], a reference change of 0.015 rad for a set of different azimuth angles of  $\pi/2$  rad,  $\pi/3$  rad,  $\pi/6$  rad,  $\pi/9$  rad and  $\pi/18$  rad are applied.

The azimuth responses of the PI controller proposed by Panchal et al. [2010] and the proposed QBPI controller for a reference change of 0.015 rad for a set of different azimuth angles are shown in Figures 12 and 13, respectively, where  $\tau_d = 0$  min and  $\Delta\theta_{azi}(t) = \theta_{azi}(t) - \theta_{azi}(0)$ . In comparison, the proposed QBPI controller azimuth responses converge to the nominal operating point of  $\pi/2$  rad than those of the PI controller proposed by Panchal et al. [2010].

Table 3: LFM Simulation Parameters

Parameter	Value
$r_{azi}$	$\pi/12 + 0.015$ rad
$r_{inc}$	$\pi/12 + 0.015$ rad
$K_{dls}$	$8^\circ/100$ ft
$V_{rop}$	200 ft/hr
$\theta_{azi}$	$\pi/12$ rad ( $15^\circ$ )
$\theta_{inc}$	$\pi/12$ rad ( $15^\circ$ )
$k_{pi}$	0.15
$V_{tr}$	$0.5^\circ/100$ ft
$V_{dr}$	$1^\circ/100$ ft
$\tau_d$	4.5 min
$d_t$	14.997 ft
$k_{ia}$	0.01
$k_{pa}$	0.13
$k_{ii}$	0.01

Figure 11: Simulink diagram of LFM simulation scheme for QBPI controller



Therefore, the proposed QBPI controller yields more invariant azimuth responses over broader degree of the directional drilling tool applications, than the PI controller proposed by Panchal et al. [2010].

To analyse the deleterious impacts of time delay on the feedback measurements and disturbances relating to the performance and stability of the directional drilling tool, the azimuth and inclination responses to step changes, from  $\pi/12$  rad to  $\pi/12 + 0.015$  rad and from  $\pi/12$  to  $\pi/12 + 0.015$  rad, respectively, of the PI controller proposed by Panchal et al. [2010] and the proposed QBPI controller are shown in Figures 14 and 15, respectively.

As shown in Figure 14, the attitude response of the PI controller proposed by Panchal et al. [2010] exhibits oscillations. Thus, the attitude response do not converge to the desired azimuth and inclination angles of  $\pi/12 + 0.015$  rad and  $\pi/12 + 0.015$  rad, respectively, as the PI controller proposed by Panchal et al. [2010] is incapable to deal with the deleterious impacts of the time delay of up to 4.5 min on the feedback measurements, turn rate bias disturbance of

Figure 12: PI controller azimuth responses

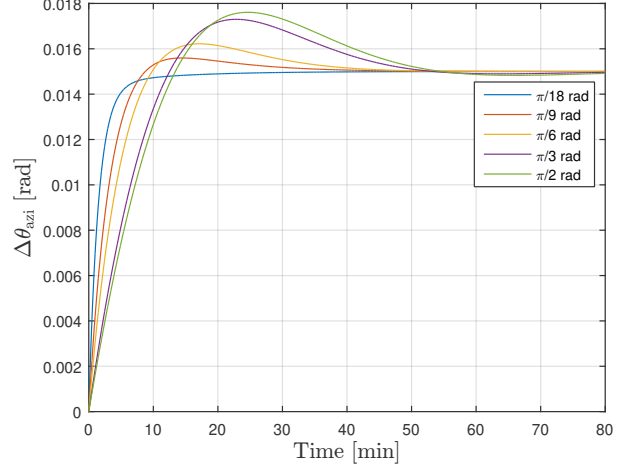
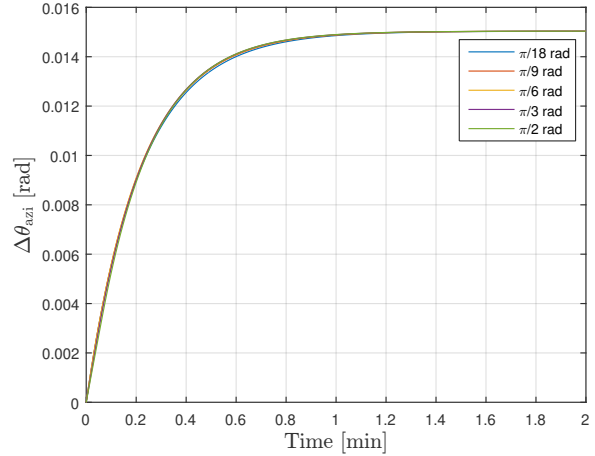


Figure 13: QBPI controller azimuth responses



up to  $0.5^\circ/100$  ft and drop rate disturbance of up to  $1^\circ/100$  ft.

As shown in Figure 15, for the proposed BPI controller, the attitude responses of the directional drilling tool converges to the desired azimuth and inclination angles of  $\pi/12 + 0.015$  rad and  $\pi/12 + 0.015$  rad, respectively. Therefore, the proposed QBPI controller diminishes the deleterious impacts of the time delay of up to 4.5 min on the feedback measurements, turn rate bias disturbance of up to  $0.5^\circ/100$  ft and drop rate disturbance of up to  $1^\circ/100$  ft relating to the performance and stability, than the PI controller proposed by Panchal et al. [2010].

The azimuth and inclination errors for the proposed QBPI controller are shown in Figure 16. Within 72 min, the proposed QBPI controller is capable of con-

Figure 14: PI controller attitude response

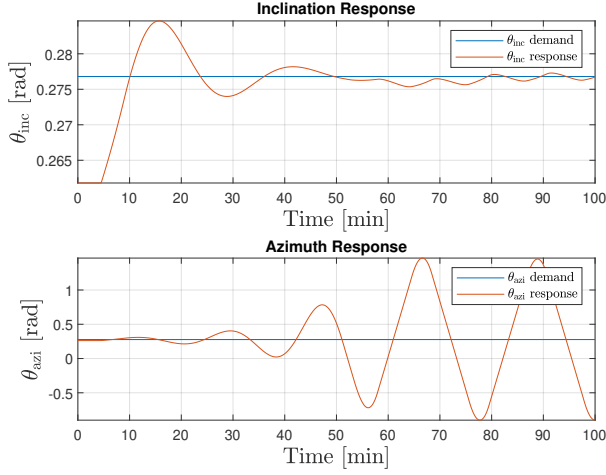
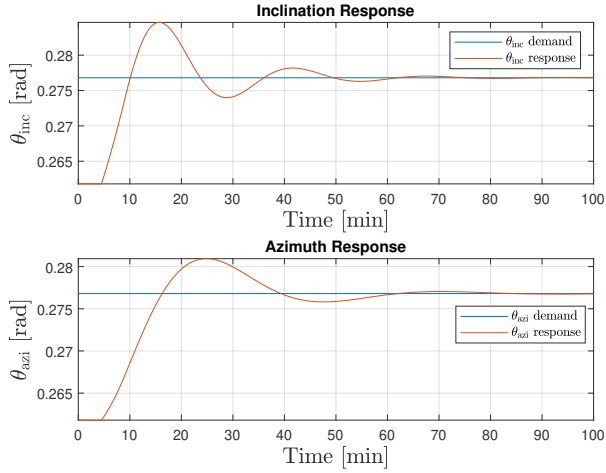


Figure 15: QBPI controller attitude response



verging the azimuth and inclination errors directly to zero.

## 7.2 High-Fidelity Model Simulation

Similar to the LFM simulation highlighted in Subsection 7.2, MATLAB/Simulink transient simulations are developed with reference to the HFM simulation scheme, shown in Figure 17, where the drilling cycle scheme (developed in Section 4) is incorporated to further investigate the effectiveness, robustness and stability of the proposed QBPI controller. The HFM simulations parameters are presented in Table 4 and they are dependent on practical engineering considerations.

For the proposed QBPI controller, the inclination

Figure 16: Attitude error for QBPI controller with LFM

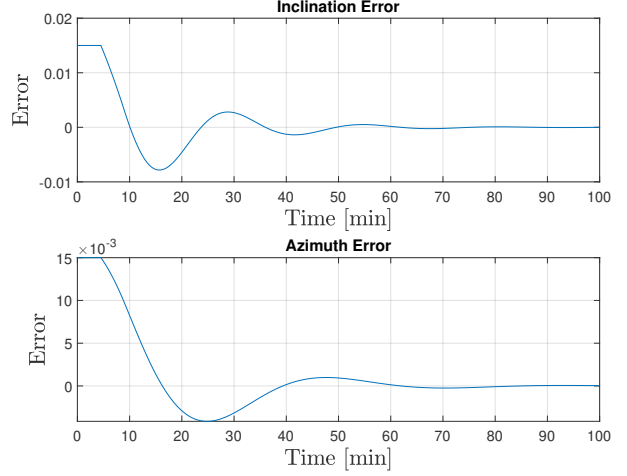


Table 4: HFM Simulation Parameters

Parameter	Value
$\theta_{inc}$	$7\pi/18$ rad ( $70^\circ$ )
$\theta_{azi}$	$7\pi/18$ rad ( $70^\circ$ )
$V_{rop}$	200 ft/hr (1.0158 m/min)
$K_{dls}$	$8^\circ/100$ ft ( $4.5809 \times 10^{-3}$ rad/m)
$r_{inc}$	$7\pi/18 + 0.015$ rad
$r_{azi}$	$7\pi/18 + 0.015$ rad
$k_{pi}$	0.15
$k_{ii}$	0.01
$k_{pa}$	0.13
$k_{ia}$	0.01
$T_a$	0.05 s ( $8.333 \times 10^{-4}$ min)
$k_p$	$1 \text{ s}^{-1}$ ( $60 \text{ min}^{-1}$ )
$k_{vp}$	0.5
$k_{vi}$	$6 \text{ s}^{-1}$ ( $360 \text{ min}^{-1}$ )
$t_{cycle}$	10 s (0.1667 min)
$\hat{\omega}_{tf}$	$2\pi$ rad/s (376.991 rad/min)
$d_t$	14.997 ft (4.5711 m)
$\tau_d$	4.5 min
$V_{dr}$	$1^\circ/100$ ft ( $5.7261 \times 10^{-4}$ rad/m)
$V_{tr}$	$0.5^\circ/100$ ft ( $2.8631 \times 10^{-4}$ rad/m)

Figure 17: Simulink diagram of HFM simulation scheme for QBPI controller

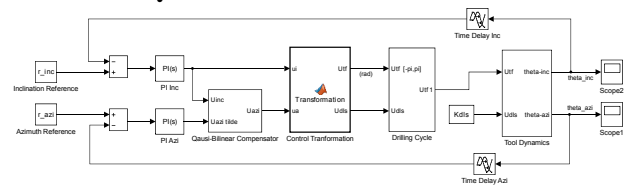


Figure 18: QBPI controller attitude response with HFM

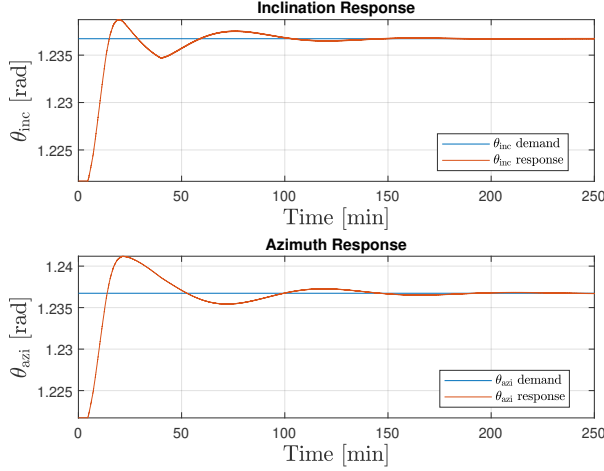
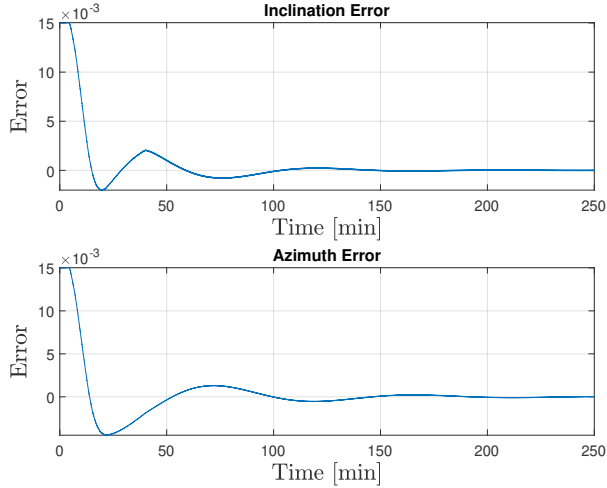


Figure 19: Attitude error for QBPI controller with HFM



and azimuth responses to step changes, from  $7\pi/18$  rad to  $7\pi/18 + 0.015$  rad and from  $7\pi/18$  rad to  $7\pi/18 + 0.015$  rad, respectively, are shown in Figure 18. The proposed QBPI controller still holds the azimuth and inclination of the directional drilling tool at the desired angles of  $7\pi/18 + 0.015$  rad and  $7\pi/18 + 0.015$  rad, respectively. Therefore, the proposed QBPI controller is robust, stable and effective to deal with the deleterious impacts of the time delay of up to 4.5 min on the feedback measurements, turn rate bias disturbance of up to  $0.5^\circ/100$  ft and drop rate disturbance of up to  $1^\circ/100$  ft and some other uncertainties (such as drilling cycle and tool actuator dynamics) in the attitude control of the directional

drilling tool.

The azimuth and inclination errors for the proposed QBPI controller are shown in Figure 19. Within 180 min, the proposed QBPI controller is capable of converging the azimuth and inclination errors directly to zero.

## 8 Conclusions

This article proposes a quasi-bilinear model of directional drilling tool. The proposed quasi-bilinear model accurately depicts the nonlinear characteristics of directional drilling tool to a greater extent than the existing linear model. Therefore, it extends the scope of appropriate performance and it is considered to be outstandingly beneficial in application to directional drilling operations. Based on the proposed quasi-bilinear model, a quasi-bilinear controller (QBPI controller) is designed for the attitude control of directional drilling tool.

The proposed QBPI control system is an LTI system and it is shown to be exponentially stable. The proposed QBPI controller is capable of holding the attitude of the directional drilling tool at the desired azimuth and inclination angles, yields invariant azimuth responses over broader scope of directional drilling operations and outstandingly diminishes the deleterious impacts of the time delay of up to 4.5 min on the feedback measurements, turn rate bias disturbance of up to  $0.5^\circ/100$  ft and drop rate disturbance of up to  $1^\circ/100$  ft and some other uncertainties (such as drilling cycle and tool actuator dynamics) in the attitude control of the directional drilling tool.

The proposed QBPI controller is reasonably simple and it can with ease be applied in the directional drilling tools for more effective drilling, field development and the improvement of the potential of accessing difficult reservoirs.

Furthermore, this article presents the development of a drilling cycle scheme which captures the drilling cycle and toolface actuator dynamics of the directional drilling tool, and it is suitable for High-Fidelity Model (HFM) simulation analyses with respect to the attitude control of the directional drilling tool. The servo-velocity and servo-position loops of the toolface servo-control architecture for the drilling cycle scheme are proven to be robustly stable using Kharitonov's Theorem.

Stability proof of the proposed QBPI controller with measurement delay remains an open problem.

## References

- R. Baker. *A Primer of Oilwell Drilling*. The University of Texas at Austin in cooperation with International Association of Drilling Contractors, Texas, USA, 5th (revised) edition, 1996.
- M. T. Bayliss and J. F. Whidborne. Mixed uncertainty analysis of pole placement and  $H_\infty$  controllers for directional drilling attitude tracking. *Journal of Dynamic Systems, Measurement, and Control*, 137(12):121008, October 2015.
- M. T. Bayliss, I. J. Inyang, and J. F. Whidborne. Application of LQG control to attitude control of directional drilling. In *24th International Conference on Systems Engineering*, Coventry, UK., 2015.
- C. Bruni, G. DiPillo, and G. Koch. Bilinear systems: An appealing class of nearly linear systems in theory and applications. *IEEE Transactions on Automatic Control*, AC-19(4):334–348, August 1974.
- F. M. Callier and C. A. Desoer. *Linear System Theory*. Springer Verlag, New York, 1991.
- C. Cockburn, J. Matheus, and K. L. P. Dang. Automatic trajectory control in extended-reach wells. In *SPE Middle East Oil and Gas Show and Conference*, Manama, Bahrain, 2011.
- S. Devereux. *Drilling Technology in Nontechnical Language*. PennWell Corporation, OK, 1999.
- J. Genevois, J. Boulet, C. Simon, and C. Reullon. Gyrostab project: The missing link azimuth and inclination mastered with new principles for standard rotary BHAs. In *SPE/IADC Drilling Conference*, Amsterdam, Netherlands, 2003.
- C. Gu. QLMOR: A projection-based nonlinear model order reduction approach using quadratic-linear representation of nonlinear systems. *IEEE Transactions on Computer-Aided Design of Integrated Circuits and Systems*, 30(9):1307–1320, Sept 2011.
- I. Inyang, J. F. Whidborne, and M. T. Bayliss. Directional drilling attitude control with input disturbances and feedback delay. In *IFAC-PapersOnLine*, volume 50, pages 1409–1414, 2017. doi: j.ifacol.2017.08.246. 20th IFAC World Congress.
- I. J. Inyang. *Attitude Control of Directional Drilling*. PhD thesis, Cranfield University, Cranfield, UK, 2017.
- I. J. Inyang and J. F. Whidborne. Applying a modified Smith predictor-bilinear proportional plus integral control for directional drilling. In *IFAC Control Conference Africa*, Johannesburg, South Africa, 2017.
- I. J. Inyang and J. F. Whidborne. Bilinear modelling, control and stability of directional drilling. *Control Engineering Practice*, 82:161 – 172, 2019. ISSN 0967-0661.
- V. L. Kharitonov. Asymptotic stability of an equilibrium position of a family of systems of linear differential equations. *Differentsial’nye Uravneniya*, 14(11):1483–1485, 1978.
- B. Kim and M. Lim. Robust  $H_\infty$  control method for bilinear systems. *International Journal of Control, Automation and Systems*, 1(2):171–177, June 2003.
- N. A. H. Kremers, E. Detournay, and N. van de Wouw. Model-based robust control of directional drilling systems. *IEEE Transactions on Control Systems Technology*, 24(1):226–239, 2016.
- S. Kuwana, Y. Kiyosawa, and A. Ikeda. Attitude control device and drilling-direction control device, May 1994. US Patent 5316090.
- S. Martineau, K. J. Burnham, J. A. Miniham, S. Marcroft, G. Andrews, and A. Heeley. Application of a bilinear PID compensator to an industrial furnace. In *15th IFAC World Congress on Automatic Control*, Barcelona, Spain, 2002.
- J. Matheus and S. Naganathan. Drilling automation: Novel trajectory control algorithms for RSS. In *IADC/SPE Drilling Conference and Exhibition*, New Orleans, LA, 2010.
- J. Matheus, M. Ignova, and P. Hornblower. A hybrid approach to closed-loop directional drilling control using rotary steerable systems. In *Proceedings of the 2012 IFAC Workshop on Automatic Control in Offshore Oil and Gas Production*, Trondheim, Norway, 2012.
- J. Matheus, M. Ignova, and P. Hornblower. A hybrid approach to closed-loop directional drilling control using rotary steerable systems. In *SPE Latin American and Caribbean Petroleum Engineering Conference*, Maracaibo, Venezuela, 2014.
- N. Panchal, M. T. Bayliss, and J. F. Whidborne. Robust linear feedback control of attitude for directional drilling tools. In *13th IFAC Symposium on Automation in Mining, Mineral and Metal Processing*, Cape Town, South Africa, 2010.

- N. Panchal, J. F. Whidborne, and M. T. Bayliss. Recursive variable horizon trajectory control for directional drilling using elliptical helices. In *18th IFAC World Congress*, Milano, Italy, 2011.
- N Panchal, M. T. Bayliss, and J. F. Whidborne. Attitude control system for directional drilling bottom hole assemblies. *IET Control Theory and Applications*, 6:884–892, January 2012.
- M.H. Pedersen, M. Lechner, Z.A. Pon, D. Brink, I. Abbasy, and M.R. Jaafar. Case study: Successful application of a novel conformance treatment in an extended reach horizontal well in the Al Shaheen field, offshore Qatar. In *SPE Offshore Europe Oil & Gas Conference & Exhibition*, Aberdeen, UK., 2009.
- E. J. Routh. *Dynamics of a System of Rigid Bodies*. Macmillan, London, UK, 6th edition, 1905.
- H. Schwarz and H. T. Dorissen. System identification of bilinear systems via realization theory and its application. *Control, Theory and Advanced Technology*, 5(2):137–155, June 1989.
- J. A. Short. *Introduction to Directional and Horizontal Drilling*. PennWell Publishing Company, OK, 1993.
- C. K. Tse and K. M. Adams. Quasi-linear modelling and control of DC-DC converters. *IEEE Transactions on Power Electronics*, 7(2):315–325, 1992.
- N. van de Wouw, F. H. A. Monsieurs, and E. Detournay. Dynamic state-feedback control of nonlinear three-dimensional directional drilling systems. *IFAC-PapersOnLine*, 49(18):85–90, December 2016.
- B. A. White, L. Bruyere, and A. Tsourdos. Missile autopilot design using quasi-LPV polynomial eigenstructure assignment. *IEEE Transactions on Aerospace and Electronic Systems*, 43(4):1470–1483, 2007.
- L. Yinghui and S. Yinao. Automatic inclination controller: A new inclination controlling tool for rotary drilling. In *IADC/SPE Drilling Conference*, New Orleans, LA, 2000.
- T. Yonezawa, E.J. Cargill, T.M. Gaynor, J.R. Hardin, R.T. Hay, A. Ikeda, and Y. Kiyosawa. Robotic controlled drilling: A new rotary steerable drilling system for the oil and gas industry. In *IADC/SPE Drilling Conference*, Texas, USA., 2002.